Phenylalanine Ring Dynamics by Solid-State ^2H NMR

C. M. Gall, J. A. DiVerdi, and S. J. Opella*

Contribution from the Department of Chemistry, University of Pennsylvania, Philadelphia, Pennsylvania 19104. *Received January 26, 1981*

Abstract: Quadrupole echo ^2H NMR spectra of [$^2H_5$]-phenylalanine in polycrystalline form and incorporated into the coat protein of the filamentous bacteriophage fd demonstrate that the aromatic rings are undergoing rapid 180° flips about their C_β–C_γ bond axis. The ^2H NMR powder patterns from the δ and ϵ C–D bonds of [d_5]-Phe in both samples are in the fast exchange limit for this two-site jump model of motion. The rate of flipping is fast compared with 0.2 MHz. The results are incompatible with diffusional rotation occurring on this time scale.

I. Introduction

The motions of aromatic amino acid side chains in proteins have received a great deal of attention.[1] Not only do the dynamics of these groups have an important effect on their biological functions, but the bulk of these rings implies that their individual motions influence and are influenced by the location and motions of many other residues of the protein.

Phenylalanine and tyrosine rings have C_2 symmetry and an obvious path for internal motion, the C_β–C_γ bond axis. Nearly all of the experimental data concerning the intramolecular motions of Phe and Tyr rings have come from NMR spectroscopy of proteins in solution. Around 1974, the initial evidence indicating that some of these rings in proteins are able to reorient relatively rapidly about their C_β–C_γ bond axis became available from several different NMR experiments. Natural abundance ^{13}C[2] and labeled site ^{19}F[3] relaxation studies indicated the presence of ring motions fast compared to the overall rotation of the proteins (10^7 Hz), while the analysis of high-field ^1H resonance line shapes demonstrated that motional averaging of the δ and ϵ ring positions occurred fast compared to chemical shift differences (10^2 Hz).[4-6] Subsequently, many high-resolution ^1H NMR spectra of proteins have been interpreted in terms of individual Phe or Tyr rings being completely immobile or undergoing reorientation about their C_β–C_γ bond axis. The latter conclusion is reached when the high-resolution ^1H NMR spectrum has two doublets for a Tyr ring or two triplets and one doublet for a Phe ring, since these distinctive patterns can only occur when the chemical shift differences for both sides of a ring in an asymmetric protein environment are averaged by motion about the C_β–C_γ-symmetry axis of the ring.

There are two limiting cases for intramolecular aromatic ring reorientation: (1) *jumps* or 180° flips between two indistinguishable sites, where the residence times are long compared to the transit times; (2) continuous *rotation*, where the rings undergo unhindered diffusion around the C_β–C_γ bond. ^1H NMR line-shape analysis does not distinguish between rotational diffusion and jump modes of motional averaging. However, in discussions of high-resolution ^1H NMR spectral data, it has always been argued that the motional averaging is the result of 180° ring flips rather than rotations. This reasonable interpretation has been based on the premise that the bulk of the aromatic rings would severly hinder rotational motion within the closely packed protein interior. The ^{13}C and ^{19}F relaxation data are consistent with ring rotations, but do not rule out the presence of flips, and have been interpreted in terms of relatively small amplitude librations. Computer simulations of protein dynamics suggest that flips between equilibrium positions occur, but only with alteration of a large part of the surrounding structure.[7]

Solid-state NMR is an alternative spectroscopic approach to the study of molecular dynamics. In addition, it allows the investigation of crystalline materials and supramolecular structures such as nucleoprotein or membrane–protein complexes in solution. In general, NMR spectra of solids reflect the anisotropic character of nuclear spin interactions that are described by second rank tensors.[8] The actual resonance line shapes arise from dipolar, chemical shift, or quadrupolar interactions, depending on the nucleus and other experimental conditions. The spectral data are strongly affected by molecular motions, and by arranging situations, such as in crystals, where only intramolecular motions are possible, very detailed information about specific processes can be obtained.

By studying molecules with ^2H substituted for ^1H and obtaining ^2H NMR spectra with the quadrupole echo pulse sequence,[9] ^2H quadrupole powder patterns provide the experimental data which can be compared with calculated spectra. Solid-state ^2H NMR has been used to characterize the dynamics of a number of small molecules[10-13] and polymers.[14,15] Many studies of membrane bilayers have utilized ^2H-labeled lipids as spectroscopic probes,[16] and recently the existence of gauche-trans jump motion in lipids has been recognized based on ^2H NMR line-shape analysis[17] similar to that used here. Collagen labeled with deuterium has been studied by ^2H NMR and found to have methyl side chains undergoing both rotational and jump motions.[18,19]

fd virus is a 900 nm × 9 nm filament with its DNA packed within a tube of protein. The virus coat consists of 2700 identical 5000 MW protein subunits, each of which has three Phe residues. We are studying the structure, dynamics, and assembly of this nucleoprotein complex by NMR.[20-23] Solid-state ^{31}P NMR of

(1) Gurd, F. R. N.; Rothgeb, T. M. *Adv. Protein Chem.* **1979**, *33*, 74-166.
(2) Opella, S. J.; Nelson, D. J.; Jardetzky, O. *J. Am. Chem. Soc.* **1974**, *96*, 7157-7159.
(3) Hull, W. E.; Sykes, B. D. *J. Mol. Biol.* **1975**, *98*, 121-153.
(4) Campbell, I. D.; Dobson, C. M.; Williams, R. J. P., *Proc. R. Soc. London., Ser. B* **1975**, *189*, 503-509.
(5) Wuthrich, K.; Wagner, G. *FEBS Lett.* **1975**, *50*, 265-268.
(6) Snyder, G. H.; Rowan, R.; Karplus, S.; Sykes, B. D. *Biochemistry* **1975**, *14*, 3765-3777.
(7) McCammon, J. A.; Karplus, M. *Biopolymers* **1980**, *19*, 1375-1405.
(8) Mehring, M. "High Resolution NMR Spectroscopy in Solids"; Springer-Verlag: New York, 1976.
(9) Davis, J. H.; Jeffrey, K. R.; Bloom, M.; Valic, M. I.; Higgs, T. P. *Chem. Phys. Lett.* **1976**, *42*, 390-394.
(10) Chiba, T. J. *Chem. Phys.* **1962**, *36*, 122-1126.
(11) Soda, G.; Chiba, T. J. *Chem. Phys.* **1969**, *50*, 439-455.
(12) Pschorn, O.; Spiess, H. W. *J. Magn. Reson.* **1980**, *39*, 217-228.
(13) Boden, N.; Clark, L. D.; Hanlon, S. M.; Mortimer, M. *Faraday Symp. Chem. Soc.* **1978**, 109-123.
(14) Hentschel, R.; Spiess, H. W. *J. Magn. Reson.* **1979**, *35*, 157-162.
(15) Hentschel, D.; Sillescu, H.; Spiess, H. W. *Makromol. Chem.* **1979**, *180*, 241-249.
(16) Seelig, J. *Q. Rev. Biophys.* **1977**, *16*, 353-418.
(17) Huang, T. H.; Skarjune, R. P.; Wittebort, R. J.; Griffin, R. G.; Oldfield, E. *J. Am. Chem. Soc.* **1980**, *102*, 7377-7379.
(18) Jelinski, L. W.; Sullivan, C. E.; Torchia, D. A. *Nature (London)* **1980**, *284*, 531-534.
(19) Jelinski, L. W.; Sullivan, C. E.; Batchelder, L. S.; Torchia, D. A. *Biophys. J.* **1980**, *32*, 515-530.
(20) Opella, S. J.; Cross, T. A.; DiVerdi, J. A.; Sturm, C. F. *Biophys. J.* **1980**, *32*, 531-548.
(21) DiVerdi, J. A.; Opella, S. J. *Biochemistry* **1981**, *20*, 280-284.
(22) Cross, T. A.; Opella, S. J. *Biochem. Biophys. Res. Commun.* **1980**, *92*, 478-484.

0002-7863/81/1503-5039$01.25/0

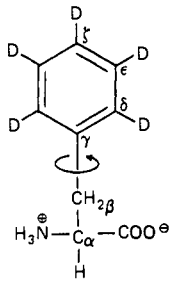

Figure 1. Structure of $[d_5]$-Phe.

concentrated virus solutions shows that the DNA is immobile on the 10^4-Hz NMR time scale.[21] Therefore, solid-state ^2H NMR spectra of fd samples where $[d_5]$-Phe has been biosynthetically incorporated into the coat proteins will reflect the intramolecular motions of these aromatic side chains.

II. Experimental Section

Samples. L-[2,3,4,5,6-$^2H_5$]Phenylalanine ($[d_5]$-Phe) was prepared from L-phenylalanine by exchange with 85% $^2H_2SO_4$ as described by Matthews et al.[24] The experimental samples were recrystallized from H_2O.

$[d_5]$-Phe labeled fd was obtained by infecting *E. coli* grown on a standard defined growth medium supplemented with $[d_5]$-Phe.[25] The virus was purified from the growth media after removal of the bacterial cells by polyethylene glycol precipitation and cesium chloride step gradient centrifugation.[23] After extensive dialysis against H_2O, the virus was concentrated by centrifugation and repeatedly exchanged with deuterium depleted water (Aldrich).

Spectroscopy. The ^2H NMR spectra were obtained on a homebuilt spectrometer with a 5.8-T magnet and a ^2H resonance frequency of 38.4 MHz. The probe was a single coil solenoid design. $\pi/2$ pulses were 2–2.5 μs in duration. The interval between $\pi/2$ pulses of the quadrupole echo sequence was 50 μs for the experimental spectra showing the figures. Spectra obtained with pulse spacings between 20 and 70 μs have essentially the same line shapes. Spectra were obtained by complex Fourier transformation of single sideband free induction decays.

III. Results and Discussion

Deuterium has a relatively large quadrupole coupling constant and a relatively small gyromagnetic ratio. Therefore, line shapes and relaxation properties of ^2H resonances are determined almost exclusively by the nuclear quadrupole interaction. By organic synthesis C–D bonds can replace C–H bonds at specific sites of molecules, thus ^2H NMR offers highly selective information in spite of limited chemical shift resolution.

The quadrupole spin interaction arises from the electrostatic interaction of the ^2H nuclear quadrupole moment with the electric field gradient of the C–D bond.[26] The electric field gradient is characterized by a symmetric second rank tensor $\hat{V}$ with principal elements $|V_{zz}| > |V_{yy}| > |V_{xx}|$ and $\sum V_{ii} = 0$ in the molecule frame principal axis system where V_{zz} is along the C–D bond, V_{yy} is perpendicular to the plane of the ring, and V_{xx} is orthogonal to these two axes. Since deuterium has nuclear spin quantum number $I = 1$, there are two allowed transitions between spin states $-1 \rightarrow 0$ and $0 \rightarrow +1$ resulting in two resonance frequencies symmetric about zero. The angular anisotropy of $\hat{V}$ means that the resonance frequencies depend on the orientation of the C–D bond with respect to the applied magnetic field.

Static Powder Patterns. Powder pattern line shapes for rigid C–D bonds are calculated from the static quadrupole coupling constant, e^2qQ/h, and asymmetry parameter, η, by taking into account the probability density of all orientations of the electric field gradient tensor with respect to the applied magnetic field. The powder pattern line shape for a molecule with a single C–D bond is the sum of two separate powder patterns, one for each of the two allowed transitions. The two constituent powder patterns are identical except for being reversed relative to zero frequency; their superposition gives the line shape shown in Figure 2 which has three pairs of spectral discontinuities, the frequencies of which are given by eq 1 in terms of the principal elements of $\hat{V}$ where $V_{zz} = {}^3/_4(e^2qQ/h)$ and $\eta = (V_{xx} - V_{yy})/V_{zz}$.

$$\nu_1 = \pm V_{xx} = \pm\frac{3}{8}\frac{e^2qQ}{h}(1-\eta)$$
$$\nu_2 = \pm V_{yy} = \pm\frac{3}{8}\frac{e^2qQ}{h}(1+\eta) \qquad \nu_3 = \pm V_{zz} = \pm\frac{3}{4}\frac{e^2qQ}{h} \tag{1}$$

A range of static quadrupole coupling constants have been reported for aromatic C–D bonds with values for benzene between 177 and 193 kHz.[13,27-30] $[d_5]$-Phe has $e^2qQ/h = 180$ kHz and $\eta = 0.05$ as determined from the experimental powder pattern from a sample at 100 K. The calculated static powder pattern for an aromatic C–D bond is shown in Figure 3E. Figure 3F contains a broadened theoretical static powder pattern for comparison with experimental spectra. The broadening corresponds to 100 Hz of Lorentzian line width from relaxation and 4 kHz of Gaussian line width from dipolar couplings.

Powder Patterns in the Presence of Motion. NMR spectra are profoundly influenced by motion. When motions of large am-

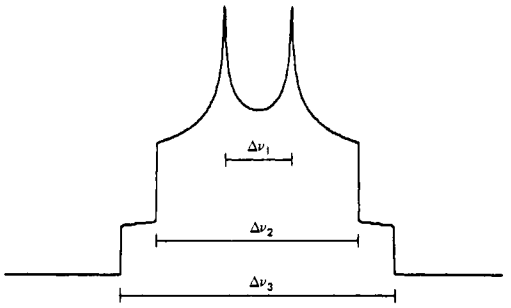

Figure 2. Calculated powder pattern for $I = 1$; shown for $\eta = 0.5$ to illustrate the three sets of discontinuities from eq 1 of the text.

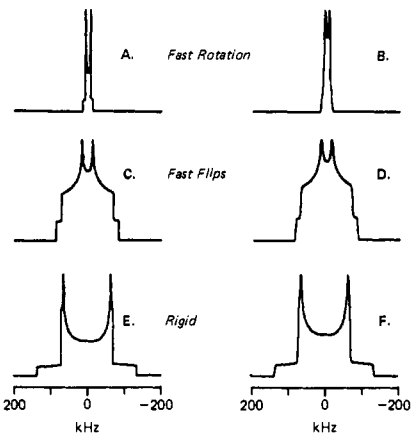

Figure 3. Calculated powder patterns for aromatic C–D bonds where $e^2qQ/h = 180$ kHz and $\eta = 0.05$. Spectra A, C, and E are unbroadened while spectra B, D, and F have 4 kHz of Gaussian and 100 Hz of Lorentzian line broadening added: (A) powder pattern averaged by fast rotation about the C_β–C_γ axis ($\beta = 60°$); (B) broadened version of A; (C) powder pattern averaged by fast 180° flips about the C_β–C_γ axis ($\theta = 120°$); (D) broadened version of C; (E) static powder pattern; (F) broadened version of E.

(23) Cross, T. A.; Opella, S. J. *Biochemistry* **1981**, *20*, 290–297.
(24) Matthews, H. R.; Matthews, K. H.; Opella, S. J. *Biochem. Biophys. Acta* **1977**, *497*, 1–13.
(25) Miller, J. H. "Experiments in Molecular Genetics" Cold Spring Harbor Laboratory: Cold Spring Harbor, N.Y., 1972.
(26) Abragam, A. "The Principles of Nuclear Magnetism," Oxford University Press Oxford, 1961.
(27) Rowell, J. C.; Phillips, W. D.; Melby, L. R.; Panar, M. *J. Chem. Phys.* **1965**, *43*, 3442–3454.
(28) Barnes, R. G.; Bloom, J. W. *J. Chem. Phys.* **1972**, *57*, 3082–3086.
(29) Diehl, P.; Reinhold, M. *Mol. Phys.* **1978**, *36*, 143–149.
(30) Seidman, K.; McKenna, J. F.; Savitsky, G. B.; Beyerlein, A. L. *J. Magn. Reson.* **1980**, *38*, 229–232.

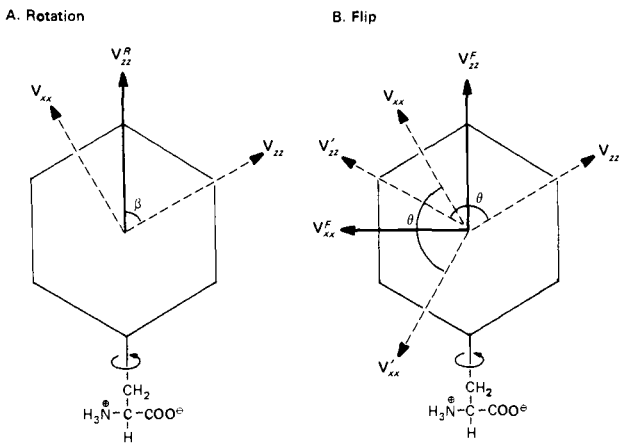

Figure 4. Illustration of motional averaging of ^2H quadrupole tensor: (A) rotation about the C_β–C_γ axis averaging V_{zz} of the C–D bond to V_{zz}^R along the axis defining $\beta = 60°$; (B) 180° flips about the C_β–C_γ bond axis between indistinguishable positions where V_{zz} and V_{zz}' are interchanged. The first exchange case gives V_{zz}^F where $\theta = 120°$.

plitude occur at rates comparable to or faster than the relevant spectroscopic time scale, the resonance line shapes are drastically altered. The time scale is determined by the dominant spin interaction; in the case of solid-state ^2H NMR, it is the frequency breadth of one of the constituent ^2H quadrupole powder patterns $(3 + \eta)^3/_4(e^2qQ/h)$ s^{-1} with a value of 0.2 MHz for aromatic C–D bonds. It is possible to calculate the powder pattern in the presence of any type of motions by taking into account the angles, amplitudes, and rates involved,[8,31-33] although in general this is difficult, time consuming, and arbitrary. However, when the rate of motion is much faster than the spectroscopic time scale, then the problem is in the "fast exchange limit" and becomes much simpler.[31] For fast motions, only the angles involved are needed for calculations of spectra for well-defined motional models.

As mentioned in the Introduction, we are concerned with motions of the aromatic ring of phenylalanine. In particular, the reorientation about the C_β–C_γ bond axis will be considered as 180° *jumps* or flips of the rings between indistinguishable positions or diffusional *rotations*. Theoretical spectra generated for the aromatic C–D bonds of phenylalanine for motionally modified powder patterns and the static spectrum are in Figure 3.

The effect of rapid diffusional rotation on ^2H NMR line shape is calculated by transforming the electric field gradient tensor from the static molecule frame principal axis system to a reference from rotating about the appropriate fixed axis with a unitary matrix expressed in terms of the Euler angles.[34] β is the angle between the static z principal axis and the rotation axis. Figure 4A shows that $\beta = 60°$ for the ϵ and C–D bonds of phenylalanine rotating about the C_β–C_δ bond axis. The rotationally averaged electric field gradient tensor, $\hat{V}^R$, has principal elements and frequencies for spectral discontinuities given by eq 2.

$$\nu_1 = \nu_2 = \pm V_{xx}^R = \pm V_{yy}^R = \pm\frac{3}{64}\left(\frac{e^2qQ}{h}\right)(1 - 3\eta)$$
$$\nu_3 = \pm V_{zz}^R = \pm\frac{3}{32}\left(\frac{e^2qQ}{h}\right)(1 - 3\eta) \quad (2)$$

The effect of rapid jumps between discrete equivalent sites on ^2H NMR line shapes is also calculated using rotation matrices; however, flip averaging differs from rotational averaging in that the orientations of the residence sites rather than the actual path of reorientation are of concern. When a molecules jumps between two equivalent sites and angle θ is defined between the z principal axes of the static electric field gradient tensor in each site. These two orientations are designated z and z' in Figure 4B, and $\theta = 120°$ for the ϵ (and δ) C–D bonds of phenylalanine for 180° flips about the C_β–C_γ bond axis. The z axis of the flip averaged tensor, $\hat{V}^F$, bisects the angle θ. The averaged x axis is perpendicular to the averaged z axis and lies in the plane formed by z and z', while the averaged y axis is perpendicular to this plane. In effect, one tensor is rotated by $\theta/2$ about the y axis of the static frame, and the other by $-\theta/2$ about the same axis. The resultant tensors are added, and the sum divided in half to account for the two populated sites. The flip averaged electric field gradient tensor, $\hat{V}^F$, has principal elements and frequencies given by eq 3.

$$\nu_1 = \pm V_{zz}^F = \pm\frac{3}{32}\frac{e^2qQ}{h}(1 - 3\eta)$$
$$\nu_2 = \pm V_{yy}^F = \pm\frac{3}{8}\frac{e^2qQ}{h}(1 + \eta) \quad (3)$$
$$\nu_3 = \pm V_{xx}^F = \pm\frac{3}{32}\frac{e^2qQ}{h}(5 + \eta)$$

Table I. ^2H NMR Spectral Parameters

aromatic C–D bond	$\pm\nu_1$, kHz	$\pm\nu_2$, kHz	$\pm\nu_3$, kHz	e^2qQ/h, kHz	η
calcd static	64.1	70.9	135.0	180.0	0.050
calcd rotation[a]	7.2	7.2	14.3	180.0	0.050
calcd for flips[b]	14.3	70.9	85.2	180.0	0.050
obsd for [d_5]-Phe at 300 K (short T_1 component)	14.0	65.3	79.3	168.1[c]	0.036[c]
calcd for flips[b]	14.1	65.3	79.4	168.1	0.036
obsd for polycrystalline [d_5]-Phe at 300 K (long T_1 component)	63.5	68.4	131.8	175.8[c]	0.037[c]
obsd for polycrystalline [d_5]-Phe at 100 K	64.1	70.8		179.9[c]	0.050[c]
obsd for [d_5]-Phe labeled fd in soln at 300 K	12.8	61.6			

[a] $\beta = 60°$ as defined in text. [b] $\theta = 120°$ as defined in text. [c] Apparent values derived from observed spectrum.

Figure 3 compares the theoretical powder patterns for aromatic C–D bonds, with and without line broadening. The three cases are static unaveraged (Figure 3E,F), averaged by rapid 180° flips about the C_β–C_γ bond axis ($\theta = 120°$) (Figure 3C,D), and averaged by rapid rotations about the C_β–C_γ bond axis ($\beta = 60°$) (Figure 3A,B). The calculated splittings are given in Table I. These three situations give markedly different splittings and line shapes for the powder patterns.

^2H NMR Experiments on Polycrystalline d_5-Phenylalanine. Figure 5 contains ^2H NMR spectra of [d_5]-Phe obtained with the quadrupole echo pulse sequence. These spectra represent a range of recycle delay times with all other experimental conditions kept constant. The spectra vary substantially in appearance as a function of recycle delay time; therefore, the T_1's of the deuterium powder patterns are distinctly nonuniform.

Substantial intensity is present in the central part of the spectra with recycle delays less than 25 ms. Therefore, much of the ^2H resonance powder pattern has short T_1. By contrast, only for long recycle delays (>5 s) is there intensity with large splittings. The spectra of Figure 5 are easily decomposed into two separate powder patterns with very different T_1's.

The short T_1 component has the characteristic shape of the powder pattern calculated for aromatic C–D bonds jumping rapidly between indistinguishable positions. Figure 6 compares an experimental short recycle delay spectrum with the broadened theoretical spectrum for 180° flip motions. The calculated and experimental line shapes and splittings are essentially identical with $e^2qQ/h = 168.1$ kHz and $\eta = 0.036$. The spectra of Figure

(31) Spiess, H. W. *Chem. Phys.* **1974**, *6*, 217–225.
(32) Alexander, S.; Baram, A.; Luz, Z. *Mol. Phys.* **1974**, *27*, 441–455.
(33) Meirovitch, E.; Freed, J. H. *Chem. Phys. Lett.* **1979**, *64*, 311–316.
(34) Mehring, M.; Griffin, R. G.; Waugh, J. S. *J. Chem. Phys.* **1971**, *55*, 746–755.

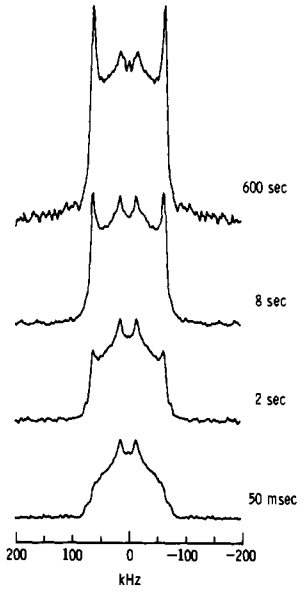

Figure 5. ^2H NMR spectra of polycrystalline $[d_5]$-Phe obtained at 38 MHz with the quadrupole-echo pulse sequence. The recycle delay is the time between initial $\pi/2$ pulses and is listed to the right of each spectrum; 1000 acquisitions of the 0.05-, 2-, and 8-s spectra, and 100 acquisitions of the 600-s spectrum were averaged. The displayed spectra are properly normalized for the number of acquisitions.

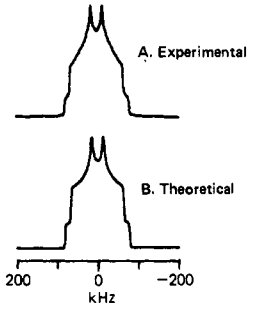

Figure 6. Comparison of short T_1 component of $[d_5]$-Phe ^2H NMR spectrum to the broadened spectrum calculated for fast 180° flips of δ and ϵ deuterons: (A) quadrupole echo ^2H NMR spectrum of $[d_5]$-Phe with 100-ms recycle delay signal averaged for 8000 scans; (B) calculated powder pattern for 180° flips of δ and ϵ C–D bonds (e^2qQ/h = 168.1; η = 0.036).

6 demonstrate that the δ and ϵ C–D bonds of $[d_5]$-Phe undergo 180° flips about the C_β–C_γ bond axis more often than 10^6 per s, since the line shape is that for the distinctive flip averaged pattern and the T_1 is short. The δ and ϵ C–D bonds have T_1 reduced significantly from the static value because the rapid jump motions generate significant spectral density near the ^2H Larmor frequency and induce efficient longitudinal relaxation.

The very long recycle delay spectrum has the long T_1 spectral component with the shape and splitting of a static powder pattern superimposed on the flip-averaged powder pattern of the short T_1 component. The intensity in the static powder pattern can arise from ξ C–D bonds, which are not affected by motions confined to the C_β–C_γ bond axis, and any molecules in the polycrystalline sample that are not undergoing 180° flips.

At 100 K polycrystalline $[d_5]$-Phe does not flip rapidly on the NMR time scale. The low-temperature spectrum has spectral discontinuities with frequencies given in Table I that correspond to e^2qQ/h = 179.9 kHz and η = 0.50. By contrast, the apparent quadrupole coupling constants and asymmetry parameters calculated from the 300 K spectra for the ξ as well as the δ and ϵ C–D bonds are reduced from these values. In addition to the large-amplitude 180° flips, the rings have motions at 300 K that are not present at 100 K. The δ and ϵ C–D sites not only are flip averaged, but also have e^2qQ/h reduced to a 168.1 kHz. This may be due to relatively small amplitude oscillations about the

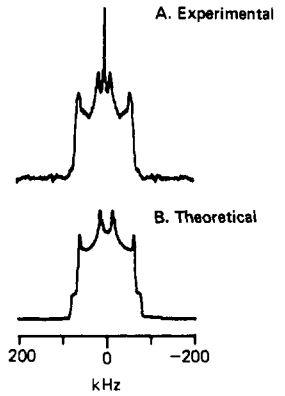

Figure 7. (A) Experimental ^2H NMR spectrum of fd labeled with $[d_5]$-Phe. (B) Theoretical ^2H NMR spectrum obtained by adding a calculated static powder pattern (e^2qQ/h = 164.3; η = 0) of area one for the ξ C–D bond and a calculated powder pattern for 180° flips of δ and ϵ C–D bonds (e^2qQ/h = 168.1; η = 0.036) of area four.

C_β–C_γ bond axis superimposed on the other ring motions which affect the outer static powder pattern.

^2H NMR Experiments on fd Phage in Solution. fd in concentrated solutions has overall rotational and translational motions that are slow on the ^2H NMR time scale.[21] Therefore, ^2H NMR spectra of specifically labeled sites of the coat protein or DNA reflect only intramolecular motions. fd where $[d_5]$-Phe has been incorporated biosynthetically gives the ^2H NMR spectrum shown in Figure 7.

The spectrum of the virus in Figure 7 is well simulated by a calculated spectrum that is the superposition of two types of ^2H NMR powder patterns with the intensity ratio of 1:4. The intensity one part is the static pattern from ξ C–D bonds and the intensity four part is the characteristically averaged pattern for the δ and ϵ C–D bonds undergoing rapid 180° flips between indistinguishable sites. The simulation of intensities suggests that all three Phe rings of the coat proteins are undergoing 180° flips.

The static line shape of the ^2H powder pattern of Figure 7 shows that the only large amplitude motions of the phenylalanine rings of fd are about the C_β–C_γ bond axis. The frequency of the outer discontinuity is 61.6 kHz which is significantly reduced from the 64.1 kHz value of a completely static C–D bond and indicates the presence of small amplitude rapid motions of these rings in directions other than about the C_β–C_γ bond axis, such as wobbling of that axis in a restricted cone as suggested by the calculations of McCammon and Karplus.[7]

The inner ^2H powder pattern of Figure 7 demonstrates that the phenylalanine rings of the coat protein in fd are executing 180° flips about their C_β–C_γ bond axis more often than 10^6 s^{-1}. The frequency of the inner discontinuities is 12.8 kHz which is somewhat reduced from the 14.3 kHz predicted for an otherwise stationary ring and the 14.0 kHz observed for polycrystalline $[d_5]$-Phe at 300 K. This may be explained by the phenylalanine rings in the protein undergoing torsional oscillations about the C_β–C_γ bond axis that are larger in amplitude than seen for polycrystalline phenylalanine.[7]

Motions of Phenylalanine Residues in Proteins. The ^2H NMR spectra of $[d_5]$-Phe labeled fd demonstrate the jump nature of phenylalanine ring motions in a native protein. This finding is in agreement with the interpretation of ^1H NMR spectra of proteins in solution.[4-6] What is remarkable about the ^2H NMR powder patterns of fd is that they put a lower limit on the rate of flips that is fast compared to 10^6 s^{-1}. This is several orders of magnitude faster than the previously determined rates or limits. The most rapid rate of ring flips actually measured is 10^4 s^{-1} at 97 °C,[35] although in general the observation of the fast exchange limit for ^1H chemical shift places a lower limit of about 10^3 s^{-1} on the process.

(35) Campbell, I. D.; Dobson, C. M.; Moore, G. R.; Perkins, S. J.; Williams, R. J. P. *FEBS Lett.* **1976**, *70*, 96–100.

The rates of ring flips for Phe and Tyr clearly vary among residues and proteins. Some rings flip very slowly or not at all ($< 10\ s^{-1}$) at a temperature where other rings in the same protein are in the fast exchange limit as described above,[5] because the ^2H NMR data of Figures 5 and 6 show that polycrystalline phenylalanine has rapidly flipping rings. With this fast dynamical process found for closely packed crystals[36] and most protein Phe and Tyr residues, it is probable that the cases of immobilized rings are to be regarded as exceptions. The larger temperature factors in the diffraction data for the ring positions of phenylalanine[36] are probably a manifestation of the same small amplitude rapid motions of the ring that reduce the apparent static quadrupole coupling constant at 300 K.

The observation of averaging of second rank tensors for analysis of dynamics works readily for quadrupolar, chemical shift, and dipolar interactions. It can apply to the rings of all the aromatic amino acids, as well as other groups of macromolecules. It is appropriate for supramolecular structures in solution such as DNA–protein complexes or membranes where the overall reorientation rate is slow. It is well suited for the analysis of dynamics of polycrystalline and amorphous solids. When the sample can be prepared with specific isotropic labels, the information surpasses that available from any other source in detail and reliability. The rates of motions can be determined through relaxation measurement on the powder patterns.

(36) Al-Karaghouli, A. R.; Koetzle, T. F. *Acta Crystallogr., Sect. B* **1975**, *31*, 2461–2465.

Acknowledgment. We thank A. Vega for helpful discussions on the interpretation of ^2H NMR spectra. This research is being supported by grants from the National Institutes of Health (GM-24266) and the American Cancer Society (NP-225). C. M.G. is being supported by a Cell and Molecular Biology Training Grant. S.J.O. is a Fellow of the A.P. Sloan Foundation (1980–1982).

On the Mechanism of Photooxygenation Reactions. Computational Evidence against the Diradical Mechanism of Singlet Oxygen Ene Reactions

K. Yamaguchi,*,† S. Yabushita,† T. Fueno,† and K. N. Houk*,‡

Contribution from the Departments of Chemistry, Faculty of Engineering Science, Osaka University, Toyonaka, Osaka 560, Japan, and University of Pittsburgh, Pittsburgh, Pennsylvania 15260. *Received May 20, 1980*

Abstract: Ab initio calculations with the STO-3G basis set and semiempirical MINDO/3 calculations at the unrestricted Hartree–Fock level show that both ab initio and semiempirical techniques predict that 1,4-diradicals formed from singlet oxygen and simple alkenes are more stable than perepoxides. Thus, both techniques now agree that perepoxides are too high in energy to qualify as viable intermediates in singlet oxygen ene reactions, as are zwitterions, for weakly polar alkenes. However, calculations on putative substituted diradical intermediates show that reactions involving such intermediates should be nonstereospecific and show significant regioselectivities. The high stereospecificity and low regioselectivity found experimentally argue strongly against the intermediacy of diradicals in this and related reactions.

The detailed electronic mechanism of singlet oxygen ene reactions with alkenes and enol ethers (Scheme I) continues to be a subject of intense interest and considerable controversy.[1] Experimental evidence has been interpreted both in favor of a perepoxide intermediate or a concerted mechanism. Theory, which should be most useful at predicting structures which cannot be examined experimentally, has cast more confusion on this subject. Dewar and Thiel reported MINDO/3 calculations which indicated that perepoxide intermediates, **1**, are formed from the reaction of simple alkenes and singlet oxygen.[2] Inagaki and Fukui preferred a perepoxide-like complex in the first stage of the reaction.[3] Harding and Goddard reported GVB–CI calculations which indicate that the perepoxide of ethylene is much higher in energy than a 1,4-diradical, **2**, resulting from formation of a single bond between one terminus of ethylene and singlet oxygen.[4] Various regiochemical and stereochemical features were interpreted in terms of biradical intermediates. Additional data, detailed elsewhere,[5] suggested to us that diradical intermediates cannot be formed in singlet oxygen ene reactions. The Harding–Goddard calculations exclude perepoxides as intermediates in singlet oxygen ene reactions and show that the 1,4-diradical is the only possible high-energy intermediate that could be formed in these reactions.

However, these authors could not exclude the possibility that these reactions are concerted, or if two-step involve only a low-

Scheme I

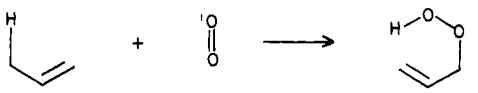

energy charge-transfer-complex-type intermediate. This intermediate must have the symmetry properties required to explain stereoselective isotope effects, but could proceed over a low-energy barrier with concerted formation of the CO and OH bonds and breaking of the CH bond. In this paper, we report some intermediate computational steps taken on the pathway to an eventual full and reliable potential energy surface for the singlet oxygen ene reaction. Our results show the following.

(1) The apparent discrepancy between the Dewar–Thiel MINDO/3 prediction[2] of the formation of a perepoxide,[3] **1**, from $^1O_2$ and ethylene and the Harding–Goddard GVB–CI prediction[4] of a diradical intermediate, **2**, for the same reaction is removed

†Osaka University.
‡University of Pittsburgh.

(1) Frimer, A. A. *Chem. Rev.* **1979**, *79*, 359. Stephenson, L. M. *Tetrahedron Lett.* **1980**, 1005. Schulte-Elte, K. H.; Rautenstrauch, V. *J. Am. Chem. Soc.* **1980**, *102*, 1738 and references therein.
(2) Dewar, M. J. S.; Thiel, W. *J. Am. Chem. Soc.* **1975**, *97*, 3978.
(3) Inagaki, S.; Fukui, K. *J. Am. Chem. Soc.* **1975**, *97*, 7480.
(4) Harding, L. B.; Goddard, W. A., III *J. Am. Chem. Soc.* **1977**, *99*, 4520.
(5) (a) Houk, K. N.; Williams, J. C.; Mitchell, P. A.; Yamaguchi, K. *J. Am. Chem. Soc.* **1981**, *103*, 949. (b) Yamaguchi, K.; Fueno, T.; Saito, I.; Matsuura, T.; Houk, K. N. *Tetrahedron Lett.* **1981**, 749.

0002-7863/81/1503-5043$01.25/0